

An Optically Driven Phased Array Antenna Utilizing Heterodyne Techniques

Marc R. Surette, Dag R. Hjelme, and Alan R. Mickelson

Abstract—A novel optically driven phased array antenna system is proposed. The system utilizes heterodyne techniques to generate the microwave carrier frequency and phases. The heterodyning at each antenna element requires three injection locked lasers. The microwave carrier frequency is determined by the order of the modulated sideband used in the injection locking scheme. A design is also presented for an integrated optical fast Fourier transform. This device can perform the necessary phase processing for both beam steering and detection of arrival angle. The recent knowledge of the noise properties of injection locked semiconductor lasers is applied to the proposed antenna system. The effect of noise on the gain, signal-to-noise ratio, and the bandwidth of the antenna system is examined. It is also shown that the performance degradation of the system, due to the noise in the lasers, is minimal, and therefore the bandwidth promise of optical drive could well be achieved with the use of heterodyne laser locking techniques.

I. INTRODUCTION

THERE are several advantages of using phased array antennas as compared to other (single transmitter) antennas [1]. Beam steering can be accomplished by varying the phase of microwave signal at each array element. This is much faster than mechanically rotating the antenna. Electronic steering allows for better stabilization of shipboard and airborne antennas. Beam formation is another important advantage. It is possible to produce a general beam footprint with extreme flexibility. Also, by appropriately controlling the amplitude and phase of the elements it is possible to reduce the power in the sidelobes. The large number of elements of a phased array antenna allows for high power since each element can be an independent transmitter. The large number of elements also allows for graceful degradation.

Even though the advantages may lead one to believe that all antennas should be phased arrays, there are several reasons which make the implementation of them difficult. First of all, the cost can become a major deterrent. In a purely microwave implementation, each antenna element must have a phase shifter and some form of amplification. Also, waveguiding in some form is required to distribute the microwave signal throughout the system. In some applications, the desired array size may be on the order of thousands of elements. Although the cost of each element may be low, such large array sizes

can make the cost of the phased array system unattractive. Packaging a large number of components obviously becomes more difficult as the number of array elements increases. The weight of the system obviously is directly related to the array size. This can be a major consideration for applications such as space based antennas. Increasing the resolution of the system requires an increase of the operating frequency, which further increases the difficulty of packaging since higher frequency antennas will have smaller array elements. A final consideration is the bandwidth of the antenna system. The direction and shape of the beam of the antenna is determined by the amplitude and phase of the electric field at each antenna element. Using Fourier analysis, it is analytically straightforward to describe the operations necessary to compute the complex field values. However, the calculations are done by digital electronics, and for large array sizes the calculations require substantial time. The computational time places a limit on the rate at which the beam can be changed, that is the bandwidth of the antenna is limited. Bandwidth is a desirable feature of an antenna system. For example, being able to alter the beam quickly allow for more complex methods to avoid detection. The disadvantages of microwave implementations of phased array antennas has led to the proposal of several architectures which utilize optics to overcome some of the problems.

The earliest proposed system which used optics was presented by Koepf [2]. The Koepf system utilizes the Fourier transforming property of a lens to provide beam-forming capabilities. This reduces the amount of digital electronics needed for the Fourier transform calculations. This results in a much faster computation time and a more compact design. Another advantage is the coherent detection scheme employed. This will allow for large array sizes since the detection process can approach the shot noise limit. However, this implementation exhibits shortcomings shared by most bulk optics systems. The thermal and mechanical instabilities of this implementation would make it unattractive for adverse environments such as airborne applications. Another disadvantage is that the microwave signal is limited to the Doppler shift that can be obtained by an acoustooptic modulator. Acoustooptic modulators are limited to a few gigahertz with a corresponding reduction in diffraction efficiency [3]. The frequency range can be extended by using magnetostatic Bragg cell [4]. The problems of the limited range of the acoustooptic cell have been addressed by using injection locked semiconductor lasers to produce higher microwave frequencies [5], [6].

Manuscript received September 24, 1991; revised March 17, 1993. This work was supported by the Office of Naval Research under Contract N00014-88-K-0685 and by the Army Research Office under Contract DAAL03-88-K-0053.

The authors are with the Department of Electrical and Computer Engineering, University of Colorado, Boulder, CO 80309-0425.
IEEE Log Number 9210184.

The stability problems in bulk optics systems encouraged the development of architectures using guided wave optics (i.e., optical fiber) for the entire system [7]–[10]. The most noticeable advantage of the fiber based architectures is the considerable reduction of the thermal and mechanical problems of the bulk optics implementation. However, the direct detection of the optical signal limits the number of elements that a given laser source can drive. Also, for large arrays, the amount of fiber required can become overwhelming. Even though the packaging problems may be less than for purely microwave implementations, it may still be a problem in fiber based systems for large arrays.

An optically controlled antenna system which has the advantages of both the bulk and fiber based system is obviously the desirable solution. The motivation has resulted in our proposal of a coherent optically driven

II. COHERENT GUIDED-WAVE IMPLEMENTATION OF OPTICALLY DRIVEN PHASED ARRAY ANTENNAS

In this section we present a discussion of a coherent guided-wave implementation of optically driven phased array antennas. First, some preliminary considerations are presented which are needed for a completed understanding of the proposed system. Modulation of semiconductor lasers is shown to have some important characteristics, one of which is the presence of both amplitude and frequency modulation simultaneously. Also, a discussion of the generation of microwave signals using injection locked semiconductor lasers is presented. Using this information, we present a description of the proposed antenna system. The discussion is mostly concerned with beam steering and direction of arrival detection.

A. Modulation of Semiconductor Lasers

The modulation response of a semiconductor laser can be expressed in terms of the laser parameters [11]. The modulation of the intensity is given by

$$\Delta P(t) = \Delta P_0 \cos(\omega_m t + \theta_P) \quad (1)$$

where

$$\Delta P_0 = \frac{G_N P_0 J_m}{\{(\omega_r^2 - \omega_m^2 + \Gamma_P \Gamma_N)^2 + 4\omega_m^2 \Gamma_r^2\}^{1/2}} \quad (2)$$

and

$$\theta_P = \arctan\left(\frac{-2\omega_m \Gamma_r}{\omega_r^2 - \omega_m^2 + \Gamma_P \Gamma_N}\right). \quad (3)$$

In these equations, ω_r is the relaxation frequency, Γ_r is the damping constant of the relaxation oscillations, and J_m is the amplitude of the modulation current. The last two parameters, Γ_P and Γ_N are damping coefficients which come from the photon and carrier rate equation, respectively. For the lasers used in our experiments, Γ_P and Γ_N have typical values of $7.5 \times 10^9 \text{ s}^{-1}$ and $1.55 \times 10^9 \text{ s}^{-1}$, respectively. Also, the relaxation oscillation damping Γ_r can be approximated by $\Gamma_r \approx \frac{1}{2}(\Gamma_P + \Gamma_N)$.

The expression for the frequency modulation response is given by

$$\Delta \nu(t) = \Delta \nu_0 \cos(\omega_m t + \theta_N) \quad (4)$$

where

$$\Delta \nu_0 = \frac{\alpha G_N J_m}{4\pi} \left(\frac{\omega_m^2 + \Gamma_P^2}{\{\omega_r^2 - \omega_m^2 + \Gamma_P \Gamma_N\}^2 + 4\omega_m^2 \Gamma_r^2} \right)^{1/2} \quad (5)$$

and

$$\theta_N = \arctan\left(\frac{\omega_m}{\Gamma_P}\right) + \arctan\left(\frac{-2\omega_m \Gamma_r}{\omega_r^2 - \omega_m^2 + \Gamma_P \Gamma_N}\right). \quad (6)$$

It is important to realize that all the sidebands of the optical spectrum can be considered phase locked to each other, a fact which is essential to the microwave generation scheme presented in the next section. Also, it is obvious that we have ignored phase noise in the previous discussion; in general, the delta functions in the optical spectrum have finite width on the order of 10 MHz.

The information presented up to this point can be used to obtain an expression for the optical spectrum of a modulated semiconductor laser. We can write an expression for a modulated optical field.

$$E = \{1 + M \cos(\omega_m t + \theta)\} e^{i\beta \sin(\omega_m t)} \quad (7)$$

where θ is the relative phase shift between the amplitude and frequency modulation, M is the amplitude modulation index, and β is the phase modulation index. The phase modulation index is defined by $\beta = 2\pi \Delta \nu / \omega_m$, where $\Delta \nu$ is the maximum frequency change, and $\omega_m / (2\pi)$ is the modulating frequency.

By convolving the AM and FM spectra and then taking the inverse Fourier transform, we can obtain a time domain expression for the modulation

$$E = \sum_{n=-\infty}^{\infty} C_n(\beta, \theta) e^{i(\omega_0 + n\omega_m)t} \quad (8)$$

where

$$C_n(\beta, \theta) = \frac{M}{2} e^{i\theta} J_{n-1}(\beta) + J_n(\beta) + \frac{M}{2} e^{-i\theta} J_{n+1}(\beta). \quad (9)$$

Equation (8) shows that the optical field spectrum is a train of delta functions at integer spacings from the optical carrier frequency.

B. Microwave Generation

As with all optical drive schemes for phased array antennas, there must be some method to generate the microwave center frequency. In the proposed system we use a microwave generation method first proposed and demonstrated by Goldberg [5]. The experimental arrangement illustrated in Fig. 1 is what we used to produce a microwave frequency.

We point out the main ideas about injection locking necessary to understand the microwave generation scheme shown in Fig. 1. When a small signal from a master laser is injected into the cavity of a second (slave) laser, it is possible for the slave to phase lock to the master. The possibility for locking

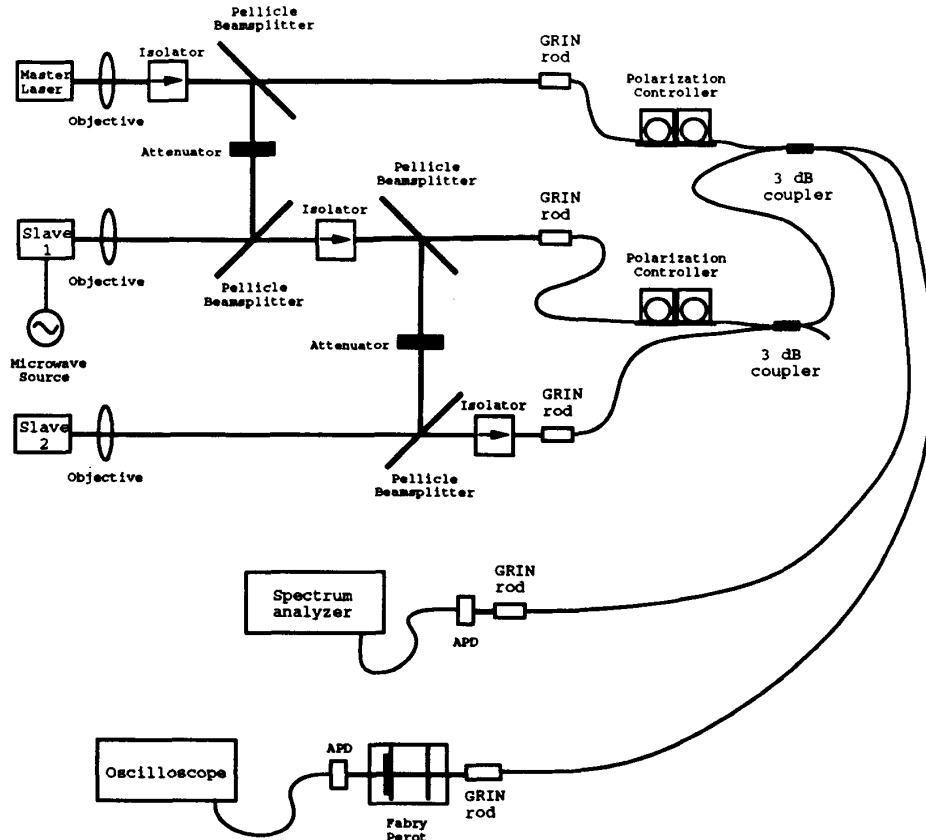


Fig. 1. Microwave generation using injection locking.

depends on the frequency difference between the master and the slave and on the amount of optical intensity injected into the slave. The conditions for injection locking to occur can be expressed by [12], [13]

$$|\Delta\omega| \leq \Delta\omega_L = f_d \sqrt{1 + \alpha^2} \sqrt{\frac{P_m}{P_s}} \quad (10)$$

where P_m/P_s represents the ratio of the optical power of the master and the slave lasers *inside* the slave cavity and f_d is the frequency difference between longitudinal modes of the slave laser. The linewidth enhancement factor α , is assumed to be 4 and f_d is assumed to be 125 GHz. Equation (10) represents the locking bandwidth $\Delta\omega_L$ of the slave laser. That is, if the frequency difference $\Delta\omega$ between the two free running lasers satisfies the above equation, then the lasers will phase lock.

Referring again to Fig. 1 we see that the master laser injects a signal into the modulated slave laser (slave 1). The modulated slave laser then injects a signal into the second slave laser (slave 2). The operating frequencies of the three lasers are illustrated in Fig. 2. The lasers used in this experiment were single mode Hitachi HLP-1600 Fabry-Perot laser diodes lasing at a wavelength of approximately $0.83 \mu\text{m}$. The output of each laser is collimated by a Newport F-L40B diode laser objective lens. The isolators shown consist of two HOYA M500 isolators in series with a half wave plate in between to

match the polarization of the beam to the input polarizer of the second isolator. The isolation obtained is approximately -70 dB. The collimated output of each laser is then coupled into a single mode fiber with a collimating GRIN rod. We used Gould 3-dB fiber couplers to obtain the heterodyne signal which was subsequently detected and displayed on a spectrum analyzer. Also, as shown, the second output of the 3-dB coupler was sent through a plane mirror Burleigh Fabry-Perot interferometer which had a variable free spectral range of approximately 15 to 400 GHz. The injection level is chosen such that the locking bandwidth of slave lasers in our experiment was much smaller than the modulating frequency. In fact, the modulating frequency was 5 GHz, whereas the locking bandwidth was approximately 500 MHz. The center frequency of the slave was injection locked to the master. The modulated laser is operated such that the second slave locks to the first-order sideband, but cannot lock to the other sidebands. All the frequency components illustrated in Fig. 2 are phase locked together since the sidebands of a modulated signal are phase locked to the carrier. Therefore, the master laser and the second slave laser are phase locked to one another and separated by the modulating frequency.

The experimental results obtained from the arrangement shown in Fig. 1 will now be discussed. In this particular

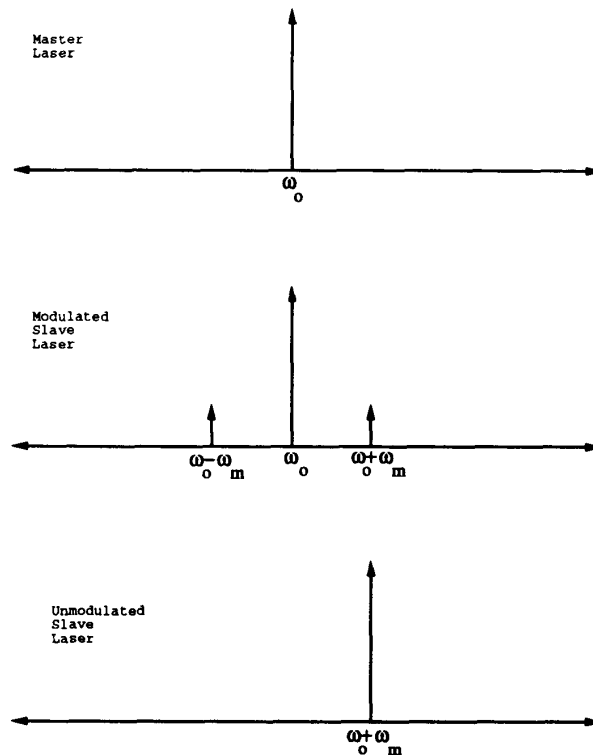


Fig. 2. Lasing frequencies of lasers for microwave generation.

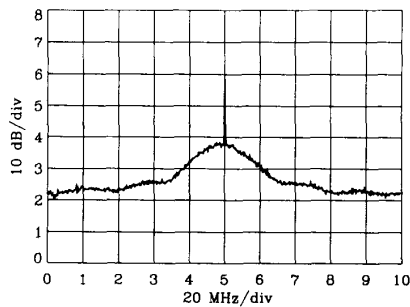


Fig. 3. Microwave signal with 100-kHz resolution.

experiment, the heterodyne signal of the master laser beating with the unmodulated slave is detected by an avalanche photodiode (APD) and displayed on a spectrum analyzer. In Fig. 3, the output of the spectrum analyzer is shown. In this figure the resolution bandwidth of the spectrum analyzer was 100 kHz and the center frequency was 5 GHz. It is clear that there is a frequency component with a narrow linewidth located at 5 GHz.

The phase locking between all the frequency components of the three lasers allows one to obtain a narrow heterodyne beat frequency. The lasers used in these experiments have linewidths of approximately 10 MHz. Therefore, when two unlocked lasers are frequency tuned to be 5 GHz apart, then the

observed beat note is roughly 20 MHz wide. This is observed by blocking the signal from the modulated laser which was used to injection lock the unmodulated slave in Fig. 1. This causes the second laser to be unlocked (phase independent) from the other two lasers. Therefore, a narrow frequency component is no longer found at 5 GHz. Also, the signal is not even centered at 5 GHz because in the free running state the master laser and the unmodulated slave are slightly further apart than 5 GHz.

C. Proposed System

Using the information presented in the previous two sections, we are now in a position to describe an optically

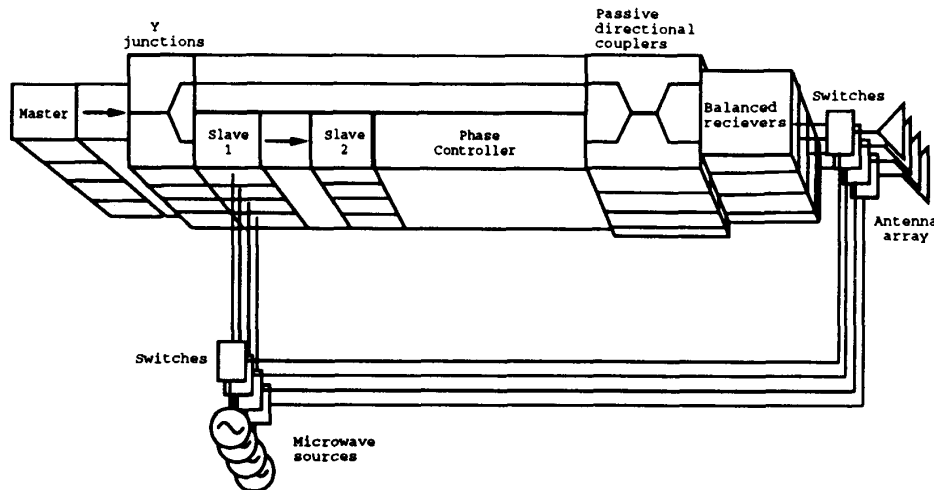


Fig. 4. Proposed phased array antenna system.

driven coherent phased array antenna system. The system uses injection locked semiconductor lasers to produce microwave signals and either a lens or an integrated optical Fourier transforming device to optically set the necessary phase shifts for beam steering and also detect direction of arrival. First, consider a single channel of the phased array system shown in Fig. 4. The single channel is very similar to the experimental arrangement of the previous section. There are a few notable differences. First, the output of the last 3-dB coupler is sent into a balanced receiver, amplified and sent to a radiating element. Second, there is a phase controller shown, used to control the microwave phase of the channel. Finally, there is a connection made, through a switch, from the modulated laser's injection current to the antenna. This connection is needed because during transmission the modulated slave is driven by a microwave source; however, when receiving a signal, the antenna element drives the modulation current. These points are discussed in more detail in the following sections.

1) *Beam Steering*: In this section we discuss the method used for beam steering the antenna system. It is understood that the beam direction of the main lobe of the antenna pattern from a phased array antenna can be controlled by applying appropriate phase at each antenna element. In fact, if a uniform progressive phase factor (linear phase taper) is used, then a simple relationship is obtained describing the beam direction. A uniform progressive phase means that some constant value $m\phi$ is added to the phase of each element, where m is the element number. Now we can write an expression which indicates the beam direction [14]

$$\phi = \frac{2\pi d}{\lambda} \cos(\theta_b) \quad (11)$$

where λ is the wavelength of the microwave field, d is the distance between adjacent elements of the array, and θ_b is the beam direction relative to a line perpendicular to the linear array. If we can obtain this progressive phase optically it would eliminate the need for microwave phase shifters. This results in simpler and lighter packaging of the system. Now, consider the

entire four-element antenna system as illustrated in Fig. 4. The lasers shown can be on a single substrate (i.e., laser arrays) but not coupled together. The master laser array must be locked to a reference frequency which can be accomplished by locking the array to the collimated output from a laser diode. The modulated slave laser array must be individually addressable. This means that the array is packaged such that a separate lead is provided for each laser in the array. Unlike the lasers, which operate independently from others in adjacent channels, the phase controller is shared between all the channels. We now discuss different types of optical components which can provide appropriate phase shifts to steer the output of the antenna.

The most obvious optical element which can provide the needed phase processing is a simple lens. Consider placing a convex lens a focal length away from the unmodulated slave laser array. If one element of the unmodulated laser array is allowed to illuminate the lens, then we know that a collimated beam is produced. Also, the angle of the collimated beam is determined by the distance of the point source from the optic axis. The angular beam provides a progressive optical phase across the inputs of the directional couplers. Thus we can express the optical signal into one arm of a passive directional coupler as

$$E_1 = e^{i((\omega_o + \omega_m)t + m\phi)} \quad (12)$$

where ω_o is the optical carrier frequency, ω_m is the microwave modulating frequency, ϕ is a constant, and m is the channel number. We also can express the other input as $E_2 = e^{i\omega_o t}$. The magnitude squared of the sum is

$$|E_1 + E_2|^2 = 2 + 2 \cos(\omega_m t + m\phi). \quad (13)$$

Therefore, the optical phase is converted to microwave phase. The output of the directional couplers can then be sent to the antenna elements to produce a beam with a direction related to ϕ , as shown in (11). To understand beam steering in the proposed system, consider the case where the modulating

current to the first slave laser array (slave 1) is removed, and that every element of the second slave array (slave 2) is lasing and illuminating the lens. At any particular input to a 3-dB directional coupler (located after the lens) there will be a sum of N different plane waves where N is the number of channels. We set the free running operating conditions of the master and slave 2 such that the beat frequency of each of the N components is different from the resonance of the antenna elements. The detected optical signal will not have a component at the antenna element resonance. Therefore, the antenna array will not transmit a signal. Now consider modulating *one* element of the first slave laser array. This causes the detected signal of the N plane waves to have one component precisely equal to the antenna resonance, and this resulting microwave beat note, including the phase information obtained from the lens, is transmitted from the antenna array. Beam steering is easily accomplished by modulating different elements of the first slave laser array. It is clear that the time necessary to achieve injection locking will directly limit the rate at which the beam direction can be changed. This rate is discussed more in the next section. Although a lens is a simple way to describe the operation of the antenna system, there are some important reasons to choose a different technique for the phase controller. As we pointed out in the introduction, the bulk optical implementations for optical drive of antenna arrays are unattractive because of thermal and mechanical stability considerations. In addition, the optical loss induced by the coupling of the collimated beam into a single mode input arm of a directional coupler would be large. This motivated us to consider equivalent phase processing in integrated optics.

We decided to approach the integrated solution in a manner similar to that of Butler and Lowe [15]. They developed a phase processing matrix which used only 3-dB couplers and phase shifters, both of which are readily available integrate optics technologies. The implementation of a Butler matrix requires placing predetermined passive phase shifters into a network of 3-dB couplers. An algorithm was developed which allowed a designer to determine the appropriate phase shifts for any general Butler matrix [16]. It was later shown by Nester that the Butler matrix and the Fast Fourier Transform (FFT) were essentially equivalent. Since the FFT and the Butler matrix are equivalent from the point of view of beam steering, we have decided to use an integrated optical FFT. This allow us to take advantage of the vast amounts of knowledge of the properties of this transform [17].

The fast Fourier transform algorithm requires only addition, subtraction, and multiplication of complex numbers. Using graphical representations of the calculations, a tree graph can be used to show the necessary calculations for a fast Fourier transform; see Fig. 5. In this figure, $W = \exp(-i2\pi/N)$ and N is the number of points in the transform. The W is a weighting factor for the complex value along a given line. Consider making this tree graph in integrated optics. First, it is clear that W^k is just a passive phase shift which is certainly possible to perform in integrated optics. This leaves only the addition and subtraction operation. However, a 3-dB coupler can be used to obtain the correct operations. Consider a general directional coupler; the relationship between the inputs and the

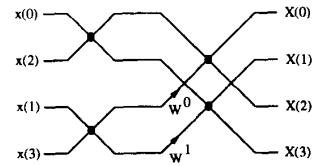


Fig. 5. Tree graph of the fast Fourier transform.

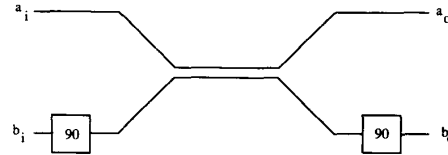


Fig. 6. Modified 3-dB directional coupler.

outputs can be expressed as [18]

$$\begin{pmatrix} a_o \\ b_o \end{pmatrix} = \begin{pmatrix} \cos\left(\frac{\Delta\beta L}{2}\right) & -i \sin\left(\frac{\Delta\beta L}{2}\right) \\ -i \sin\left(\frac{\Delta\beta L}{2}\right) & \cos\left(\frac{\Delta\beta L}{2}\right) \end{pmatrix} \begin{pmatrix} a_i \\ b_i \end{pmatrix} \quad (14)$$

where $\Delta\beta$ is the difference in propagation constants of the symmetric and antisymmetric modes of the coupling region, L is the length of the coupling region, and the “o” and “i” subscripts indicate outputs and inputs, respectively. For a 3-dB coupler, the value of $\Delta\beta L/2$ is equal to $\pi/4$. Therefore, the outputs of the 3-dB coupler are

$$a_o = \frac{1}{\sqrt{2}} (a_i - ib_i) \quad (15)$$

$$b_o = \frac{1}{\sqrt{2}} (-ia_i + b_i). \quad (16)$$

Now, to obtain the operations needed by the FFT, we only need to add passive phase shifters. The modified coupler is shown in Fig. 6. Basically, a 90-deg passive phase shift is placed on the input and output of the b channel. The resultant coupler performs the following calculations:

$$a_o = \frac{1}{\sqrt{2}} (a_i + b_i) \quad (17)$$

$$b_o = \frac{1}{\sqrt{2}} (a_i - b_i). \quad (18)$$

Apart from a constant scaling factor, the operations are exactly those required for the FFT. The design of the integrated optical FFT can be modeled directly from the tree graph of Fig. 5. It is an interesting point to consider the fact that the tree graph has intersecting lines. It is this point which limited the use of the Butler matrix in microwave antenna designs since there is no simple way to cross microstrip. However, the intersecting channels do not pose a problem in the integrate optical implementation. Unlike microstrip, if the intersecting angle of two optical channel waveguides is large enough, the resulting crosstalk is negligible. For example, two channels intersecting at an angle of 3.3 deg has roughly -15 dB crosstalk [19]. At angles on the order of 10 deg one can ignore the crosstalk.

2) *Direction of Arrival*: Obviously if an antenna system could only transmit signals it would not be extremely useful. Therefore, in this section we describe how the proposed system can detect the direction of arrival of an incoming microwave signal. In this mode of operation the microwave signal received on the antenna elements is used to modulate the slave laser array. The modulation current is given by

$$\Delta J(t) = J_m \cos(\omega_m t + m\phi) \quad (19)$$

where m is the channel number, ϕ is a constant phase determined by the direction of arrival, and ω_m is the microwave frequency. Generalizing (8), the optical field can be expressed as

$$E = \sum_{n=-\infty}^{\infty} C_n(\beta, \theta) e^{i[(\omega_o + n\omega_m)t + nm\phi]} \quad (20)$$

where $C_n(\beta, \theta)$ is a complex constant which we assume has a small variance for different channels. This is justified by considering the factors that determine this complex number. The θ dependence is related to the intrinsic phase difference between the intensity and frequency modulation of the laser, and since the lasers are on the same substrate, we can assume that θ will be very similar for all the lasers of the array. Also, for the experiments discussed in this section we noticed only a small second harmonic sideband which indicated that the phase modulation index was close to zero. This means that the $C_n(\beta, \theta)$ is approximately equal to 1 and that the effect of θ is not very important. Therefore, we can conclude that for our purposes $C_n(\beta, \theta)$ is a constant which is the same for all channels of the array and it can be ignored for the remainder of the discussion.

Assume the unmodulated slave is injection locked to the first harmonic, then looking at (20) we see that the field in the m th channel is simply

$$E = e^{i[(\omega_o + \omega_m)t + m\phi]} \quad (21)$$

Now, if all the elements of the unmodulated slave are switched through the directional coupler shown in Fig. 4 they will pass through the integrated optical FFT. Transforming a progressive phase will result in a point and the position of this point will depend on the angle of the incoming beam. This is equivalent to imaging a collimated beam through a lens. Detecting the direction of arrival is very simple for the proposed system. Basically, each output of an N channel integrated optical FFT corresponds to an incident angle; therefore, the system only needs to detect the outputs of the device and no digital processing is needed.

There is one last point which needs to be presented. It is of interest to increase the microwave center frequency in some applications. This can be accomplished in the proposed system by locking the unmodulated slave laser array to higher order harmonics of the modulated slave array. Experimentally, we have locked to the 15-GHz sideband. If lasers with higher relaxation frequencies were used, and the lasers were modulated harder, it would be conceivable to generate frequencies on the order of 40 GHz. There is a tradeoff for locking to higher order harmonics. Looking at (20) we see that the phase

ϕ is multiplied by the order of the harmonic n . This means that the angle of incidence would be multiplied by n . At first appearance, one may think that this is not a problem as long as the value of n is known. However, because of the assumed periodicity of the FFT, there will be an aliasing problem if the effective angle is too large. The system can still be used as long as during the transmit mode the angle of transmission is limited. Assume that the system is capable of transmitting at angles of $\pm\theta$ from a line perpendicular to the array. Then assume the unmodulated slave is locked to the n th-order harmonic. In order to have the system to work properly, the transmitting angles must be limited to $\pm\theta/n$. In applications where higher frequencies are needed, then a collection of systems could be used in cooperation to cover all desired transmission angles.

III. EFFECTS OF LASER INJECTION LOCKING ON OPTICAL CONTROL OF PHASED ARRAY ANTENNAS

The goal of this section is to provide information on the effects of laser injection locking on the antenna system. Obviously, operating the lasers such that the antenna system works is the most important consideration. However, as pointed out in Section II, the proposed phased array antenna system is a feasible one. Therefore, performance of the antenna is the next consideration. We begin by discussing the time necessary to injection lock two semiconductor lasers. This time will directly limit the bandwidth of the antenna. We then consider the noise affects the performance of the proposed system.

A. Effect of Locking Time on Antenna Bandwidth

We discuss a simple example which shows the bandwidth limitation caused by the locking time. In this example, we make use of the illustration of the antenna system presented in Fig. 4. Consider that slave 1 is modulated at a frequency of 5 GHz. We know that the resultant beat frequency obtained from heterodyning slave 2 and the master will be precisely equal to 5 GHz. If slave is no longer modulated, then the beat note will have a frequency different than 5 GHz. This is because when slave 1 is unmodulated, there is no sideband for the second slave to lock to. Therefore, slave 2 and the master are no longer phase locked and the two lasers will have a beat frequency different than 5 GHz. For this example, let us assume that this unlocked beat frequency is 5.5 GHz. If the antenna elements are resonant at 5 GHz and have a frequency pass band of 100 MHz, then we see that when the beat frequency is 5.5 GHz; the output of the antenna element is negligible. Therefore, it is possible to send microwave pulse trains from the antenna array simply by pulse modulating the microwave source. We have found that switching rate between a locked and unlocked state, for the lasers used in our experiment, is approximately 500 MHz [20]. In fact, the bandwidth will be roughly 10% of the relaxation frequency for typical semiconductor lasers. Therefore, for our example, the bandwidth would be limited by the 100-MHz bandwidth of the antenna element. If the bandwidth of the antenna element were increased, then the limitation due to the injection locking would become important. However, achieving 10% bandwidth

with a resonant antenna element is approximately the limit one can achieve; thus the limitation due to the injection locking time does not significantly constrain the antenna designer.

B. Effect of Relative Phase Noise

The relative phase between the master and slave lasers is not a constant. The random fluctuations in both lasers cause the steady state relative phase to be a random variable [20]. The fact that the relative phase is not constant in the injection locked state will cause degradation of the antenna system performance. However, we know that the variance of the relative phase distribution can be reduced by detecting the optical beat frequency with a finite bandwidth detector. Therefore, it is possible to achieve desired antenna system performance at the expense of system bandwidth.

3.2.1. Transmission of the Microwave Signal: During transmission, a progressive phase is placed on successive elements of the antenna array resulting in a beam propagating in a particular direction. The main lobe of this beam has a certain width which is dependent on the microwave frequency and spacing of the antenna elements. The antenna gain can be defined as the comparison of power transmitted into the solid angle of the main lobe compared to the power in that same solid angle if the antenna emitted uniformly over 4π .

Consider the effect of having a phase error at each antenna element. Obviously, the main lobe of the antenna will no longer be the same as in the ideal case of no noise. The effect of the noise will be to broaden the main lobe of the antenna which causes a degradation in the gain of the antenna. The degradation can be expressed as [1]

$$\frac{G}{G_0} = \frac{1}{1 + \langle \Delta\psi^2 \rangle} \quad (22)$$

where $\Delta\psi$ is the phase error described by a Gaussian distribution, and G_0 is the gain of the antenna in the absence of phase noise. We have derived an expression for $\langle \Delta\psi^2 \rangle$ which depended on the bandwidth of the optical detector used to detect the beat frequency of the two injection locked semiconductor lasers [20]

$$\langle \Delta\psi^2 \rangle = \frac{2(\Delta\nu_m + \Delta\nu_s)}{\pi\Delta f_L\sqrt{1-k^2}} \arctan\left(\frac{B}{\Delta f_L\sqrt{1-k^2}}\right) \quad (23)$$

where B is the detector bandwidth in hertz, $\Delta\nu_m$ and $\Delta\nu_s$ are the linewidths of the free running master and slave lasers in Hertz, and $k = \Delta\omega/\Delta\omega_L$. As expected, as the bandwidth of the detector is reduced the normalized gain degradation approaches one. However, the bandwidth of the detector directly limits the bandwidth of the antenna system. In fact, the bandwidth of the system is equal to the bandwidth of the detector if it is less than the bandwidth limit caused by the locking time.

In Fig. 7 we show a plot of the normalized gain degradation as a function of detector bandwidth. In creating this plot, we assumed a frequency detuning of 200 MHz and a locking bandwidth of 500 MHz. As can be seen from the plot, the degradation due to the phase noise is small. In the worst case (infinite detector bandwidth) the degradation is approximately

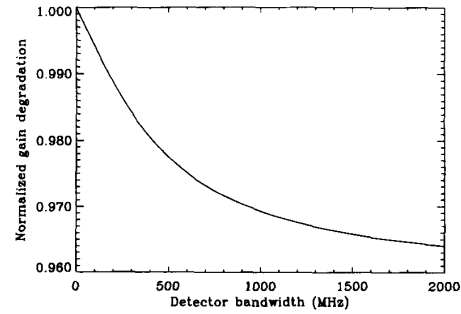


Fig. 7. Normalized gain degradation versus detector bandwidth.

to 0.96 of the maximum gain. This small degradation should not inhibit the practicality of the proposed antenna system.

3.2.2 Detection of Arrival Angle: The proposed antenna system is capable of detecting the direction of an incoming microwave signal. This is accomplished by computing a discrete Fourier transform using an integrated optical implementation of a fast Fourier transform. In an ideal case (i.e., no relative phase noise) there are N angles which when Fourier transformed result in a single output. That is, one output contains all the optical power, and the remaining outputs have zero power. However, it is clear that if there is relative phase noise on the inputs, then some of the optical power will *leak* from the correct output into other outputs. Therefore, the signal-to-noise ratio changes from the ideal value of infinity to some finite value.

We present a calculation which shows how the signal-to-noise ratio depends on the bandwidth of the detector used to detect the outputs of the Fourier transform. We first calculate the output of the discrete Fourier transform given an input field which has noise on the phase. Then the autocorrelation of the field is calculated which, by taking the Fourier transform, gives us the power spectral density. It is possible to include the effect of finite detector bandwidth by rewriting the power spectrum using (23).

First, recall that the output of a discrete Fourier transform can be expressed as

$$A_r = \sum_{k=0}^{N-1} X_k e^{-i\Omega r k} \quad (24)$$

where $\Omega = 2\pi/N$ and X_k is the input array. We can now determine what input array will give a single point output. If $X_1 = 1$ and all other X_i are zero, then the output is

$$A_r = e^{-i\Omega r}. \quad (25)$$

Therefore, because of the duality of the Fourier transform, if we let $X_k = \exp(-i\Omega r)$, we know the output will be a single point. We can express the output field of the discrete Fourier transform as

$$E_{or} = \sum_k e^{-i(\Omega k + \Delta\psi_k)} e^{-i\Omega r k} \quad (26)$$

where the input includes phase noise and the summation index is from 0 to $N - 1$. We can now express the autocorrelation

function as

$$R(\tau) = \left\langle \sum_k e^{-i(\Omega k + \Delta\psi_k(t))} e^{-i\Omega r k} \cdot \sum_m e^{i(\Omega m + \Delta\psi_m(t+\tau))} e^{i\Omega r m} \right\rangle. \quad (27)$$

This last double sum can be rewritten as the sum of diagonal terms and off-diagonal terms

$$R(\tau) = \sum_k \langle e^{-i\delta\Delta\psi_k} \rangle + \left\langle \sum_k e^{-i\Omega k(1+r)} e^{-i\Delta\psi_k} \sum_{m \neq k} e^{i\Omega m(1+r)} e^{i\Delta\psi_m} \right\rangle \quad (28)$$

where $\delta\Delta\psi = \Delta\psi(t) - \Delta\psi(t + \tau)$. We now use the fact that if θ is a Gaussian distributed random variable, to find [21]

$$\langle e^{-i\theta} \rangle = e^{-(1/2)\langle\theta^2\rangle}. \quad (29)$$

This allows us to rewrite (28) as

$$R(\tau) = \sum_k e^{-(1/2)\langle\delta\Delta\psi^2\rangle} + \sum_k e^{-i\Omega k(1+r)} e^{-(1/2)\langle\Delta\psi_k^2\rangle} \sum_{m \neq k} e^{i\Omega m(1+r)} e^{-(1/2)\langle\Delta\psi_m^2\rangle}. \quad (30)$$

Since all the inputs are assumed to have the same phase noise statistics, it is not necessary to have subscripts on the $\Delta\psi$ terms in (30). This allows us to rewrite the autocorrelation as

$$R(\tau) = N e^{-(1/2)\langle\delta\Delta\psi^2\rangle} + e^{-\langle\Delta\psi^2\rangle} \left(\sum_k \sum_m e^{-i\Omega(1+r)(k-m)} - N \right). \quad (31)$$

The double sum in (31) is recognized as the output power (since it is equal to $|E_{or}|^2$) of the Fourier transform ignoring noise. Assuming that the amplitude of each input is one, then we know that the double sum term will be equal to N^2 for the output corresponding to the input phase taper, and zero for all other outputs. We now compute the power spectral density by taking the Fourier transform of the last expression. Having the power spectrum will allow us to calculate the signal-to-noise ratio of the system. Note that the first term of the last equation is the only term which is dependent on τ . Therefore, by expanding the exponent, the Fourier transform of the first term is

$$\mathcal{F}\{e^{1/2\langle\delta\Delta\psi^2\rangle}\} \approx e^{-\langle\Delta\psi^2\rangle} \delta(\omega) + S_{\Delta\psi} \quad (32)$$

where $S_{\Delta\psi}$ is the power spectral density of the relative phase noise. The final form of the spectral density is

$$\mathcal{F}\{R(\tau)\} = S_E \approx N S_{\Delta\psi} + I_r e^{-\langle\Delta\psi^2\rangle} \delta(\omega) \quad (33)$$

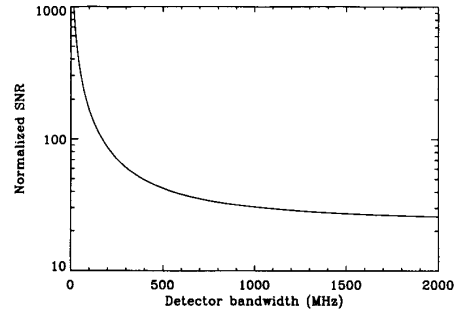


Fig. 8. Signal-to-noise ratio as a function of detector bandwidth.

where $I_r = N^2$ for the signal output channel and zero for all the others. Therefore, we can write the signal-to-noise ratio as

$$\frac{S}{N} = 1 + \frac{N e^{-\langle\psi^2\rangle}}{\int_{-\infty}^{\infty} \frac{d\omega}{2\pi} S_{\Delta\psi}} = 1 + \frac{N e^{-\langle\Delta\psi^2\rangle}}{\langle\Delta\psi^2\rangle}. \quad (34)$$

This expression can be modified to include the effects of finite detector bandwidth by changing the limits of integration. This is what was done to obtain (23). Therefore, we just need to replace the integral in (34) with (23).

The signal-to-noise ratio as shown in (34) can be explained by considering the coherence of the input. Given that the field at one particular input has a unit amplitude, then we know that the output at the correct output power will be N^2 because the N field components add coherently. On the other hand, the other channels have output power which is due to the phase noise on the input. Therefore, since the fields at these outputs do not add coherently, the output power is N . Therefore, the signal (N^2) to noise (N) ratio should scale with N , and this is the case in (34). For the worst case (infinite detector bandwidth), and assuming the same detuning and locking bandwidth as used in the last section, the signal-to-noise ratio is approximately equal to $22N$, where N is the number of channels. In Fig. 8 we show a plot of the normalized signal to noise ratio (S/N divided by the number of channels) as a function of detector bandwidth. In creating these curves, we assumed a frequency detuning of 200 MHz and a locking bandwidth of 500 MHz. As with the gain reduction, the effects of noise on the detection of arrival angle are minimal. The values of the signal-to-noise ratio shown in Fig. 8 should not present any major design obstacle to the antenna designer.

REFERENCES

- [1] M. Skolnik, *Introduction to Radar Systems*, 2nd ed. New York: McGraw-Hill, 1962.
- [2] G. A. Koepf, "Optical processor for phased-array antenna beam formation," in *Optical Technology for Microwave Applications*, vol. 477, SPIE, 1984, pp. 75-81.
- [3] C. Campbell, *Surface Acoustic Waves Devices and Their Signal Processing Applications*. Orlando, FLA: Academic, 1989.
- [4] C. Tsai and D. Young, "Magnetostatic forward volume wave based guided-wave magneto-optic Bragg cells and applications to communications and signal processing," *IEEE Trans. Microwave Theory Tech.*, vol. 38, pp. 560-570, 1990.
- [5] L. Goldberg, "Microwave signal generation with injection-locked laser diodes," *Electron. Lett.*, vol. 19, pp. 491-493, June 1983.

- [6] G. Simonis and K. Purchase, "Optical generation, distribution, and control of microwaves using laser heterodyne," *IEEE Trans. Microwave Theory Tech.*, vol. 38, pp. 667-669, 1990.
- [7] P. Sheehan and J. Forrest, "The use of optical techniques for beam-forming in phased arrays," in *Optical Technology for Microwave Applications*, vol. 477, SPIE, 1984, pp. 82-89.
- [8] J. Wallington and J. Griffin, "Optical techniques for signal distribution in phased arrays," *GEC. J. Res.*, vol. 2, no. 2, pp. 66-73, 1984.
- [9] J. Guggenmos and R. Johnson, "Fiber based phased array antennas," in *Optical Technology for Microwave Applications III*, SPIE, 1987, pp. 70-77.
- [10] S. Pappert, "Ultra-wideband direction finding using a fiber optic beam-forming processor," in *Optoelectronic Signal Processing for Phased-Arrays*, vol. 886, SPIE, 1988, pp. 239-246.
- [11] G. Agrawal and N. Dutta, *Long-Wavelength Semiconductor Lasers*. New York: Van Nostrand, 1986.
- [12] R. Lang, "Injection locking properties of a semiconductor laser," *IEEE J. Quantum Electron.*, vol. 18, pp. 976-983, June 1982.
- [13] F. Mogensen, H. Olesen, and G. Jacobsen, "Locking conditions and stability properties for a semiconductor laser with external light injection," *IEEE J. Quantum Electron.*, vol. 21, pp. 784-793, July 1985.
- [14] R. S. Elliott, *Antenna Theory and Design*. New York: Prentice-Hall, 1981.
- [15] J. Butler and R. Lowe, "Beam-forming matrix simplifies design of electronically scanned antennas," *Electron. Des.*, pp. 170-173, Apr. 1961.
- [16] W. G. Jaeckle, "Systematic design of a matrix network used for antenna beam steering," *IEEE Trans. Antennas Propagat.*, pp. 314-316, Mar. 1967.
- [17] R. N. Bracewell, *The Fourier Transform and Its Applications*. New York: McGraw-Hill, 1986.
- [18] A. Weierholt, A. Mickelson, and S. Neegard, "Eigenmode analysis of symmetric parallel waveguide couplers," *IEEE J. Quantum Electron.*, vol. 23, pp. 1689-1700, Oct. 1987.
- [19] E. E. Bergmann, L. McCaughan, and J. E. Watson, "Coupling of intersecting Ti:LiNbO₃ diffused waveguides," *Appl. Opt.*, vol. 23, pp. 3000-3003, Sept. 1984.
- [20] M. Surette, "Noise properties of injection locked semiconductor lasers: Application to optically driven phased array antennas," University of Colorado, Boulder, Ph.D. dissertation, 1991.
- [21] M. Lax, "Quantum noise VII: The rate equations and amplitude noise in lasers," *IEEE J. Quantum Electron.*, vol. 3, pp. 37-46, Feb. 1967.
- Marc R. Surette**, photograph and biography not available at the time of publication.
- Dag. R. Hjelme**, photograph and biography not available at the time of publication.
- Alan R. Mickelson**, photograph and biography not available at the time of publication.